A SYSTEMATIC STUDY FOR SELECTING AN ADEQUATE TORTUOSITY MODEL

Ali. A. Garrouch, Liaqat Ali, Fuad Qasem, and Abdullah S. Ebrahim
Petroleum Engineering Department
Kuwait University

ABSTRACT

Experimental data for molecular diffusion, electrical conductivity and capillary pressure were obtained for 14 sandstone rock samples. The four-electrode electrical measurements were used to generate rock formation factor. The centrifuge capillary pressure measurements were used to generate distribution-function curves. The coefficients of effective diffusion for a pair of helium-nitrogen gases were calculated by matching the dimensionless concentration profile obtained from the counter-current gas diffusion data to the simulated rock concentration profile obtained by solving the diffusion equation in porous media. These diffusion coefficient measurements were transformed into rock tortuosity, using various models available in the literature, and compared to corresponding values obtained from analogous electrical conductivity models. The best match occurred between tortuosities derived from diffusion data using Brakel and Heertjes model, and tortuosities derived from electrical conductivity data using Pirson's model. The matched diffusion-derived tortuosity values were then used in a simple capillary-tube model to predict sandstone rock permeability. The model adequately predicts rock permeability when adjusted by a pore geometrical factor that is a function of the volume of pore throats controlling fluid flow in porous rocks, and inversely proportional to the tortuosity squared.

INTRODUCTION

Tortuosity accounts for the fact that pore throats, responsible for flow in porous media, are not straight. Thus tortuosity is defined as the ratio of the flow path length to the sample path length. Tortuosity is an important petrographic parameter that characterizes porous media for the study of fluid flow properties. Its importance is reflected by its occurrence in rock permeability models (Panda and Lake, 1995), dielectric dispersion models for shaly sands (Garrouch and Lababidi, 1995), and even in mathematical models used to determine the characteristic relaxation time of viscoelastic fluids (Savins, 1969). The mathematical model for rock permeability presented by Panda and Lake (1995) can be rearranged to illustrate the complex relationship between tortuosity, the statistical parameters of the particle size distribution, amounts of pore-bridging, pore-lining, and pore-filling cements and their corresponding surface areas. This rearranged relationship is given by

$$t = \frac{\overline{D}_p^2 f^3 \left(g C_{D_p}^3 + 3C_{D_p}^2 + 1\right)^2}{\left\{2k(1-f)^2\left[6\frac{\left(1+C_{D_p}^2\right)(1-f_0)}{(1-f)} + \left(a_{vb}P_b + a_{vl}P_l + a_{vf}P_f\right)\overline{D}_p\left(gC_{D_p}^3 + 3C_{D_p}^2 + 1\right)\right]^2\right\}} \quad (1)$$

Here, ϕ and k are the porosity and the permeability, respectively; P_b, P_l, P_f are the amounts of pore-bridging, pore-lining, and pore filling clays, respectively, expressed as a fraction of total solid volume; a_{vb}, a_{vl}, a_{vf} are the specific surface areas of pore-bridging, lining, and filling cement, respectively; $\overline{D}_p$, C_{D_p}, and γ represent the statistical parameters of the particle size distribution, i.e. the mean grain size, its

coefficient of variation which is the mean divided by the standard deviation, and the skewness coefficient of the particle size distribution, respectively. Even though the above model gives a complete representation of the flow tortuosity of a consolidated porous medium, since it uses all the relevant permeable medium properties, its practical use is limited because of the difficulty in measuring the amount, location and type of cement crystals in a pore body. The need for an accurate and precise empirical model becomes evident.

A variety of authors postulated empirical models for tortuosity using resistivity, and molecular diffusion data. Tables 1 and 2 present a summary of the tortuosity models available in the literature. These models have so much disparity that one wonders which model should be used in characterizing a particular porous media. Their physical basis is, however, sound since electrical charge and mass transport due to diffusion in porous media are processes dependent on the geometry of the pores. The effective diffusitivity in porous media, for instance, is numerically less than the diffusitivity of molecules in the absence of the porous media. This is due to the tortuous path encountered and the changing size of constrictions of the porous media. Therefore, the effective diffusitivity of any system is characteristic of that system. Hedley et al. (1966) verified Wyllie and Spangler's assumption (1952) which stated that electrical and molecular diffusivities were equivalent. This verification, however, was performed for only porous systems composed of sintered pyrex glass, alundum, porcelain, packed activated alumina and packed glass beads. Our intention is to further verify the equivalence between electrical and molecular diffusivities for sandstone rock samples.

The purpose of this work, therefore, consists of generating molecular diffusion and four-electrode electrical resistivity data for a variety of sandstone rock samples for the purpose of estimating their corresponding tortuosity. A comparison between the two methods for estimating tortuosity is presented for the purpose of verifying if the two different experimental techniques lead to the same estimate, and for choosing adequate empirical models for tortuosity.

EXPERIMENTAL PROCEDURES

Fourteen core samples from four types of sandstone rocks were used in this study. These core samples were cut from Berea, Okesa, Tallant, and Elgin sandstone outcrops. A petrographic summary of these core samples is presented in Table 3. The core samples have an average permeability of 1024 md with a standard deviation of 885 md, and an average porosity of approximately 24% with a standard deviation of 2.7%. The Elgin sandstone is a massive to cross bedded, medium to fine grained sandstone. It is Pennsylvanian in age (Virgil Epoch) and is located in Southern Kansas and northern and central Oklahoma. The Okesa sandstone is a member of Barnsdall formation. It is fine to medium grained, overlain by shale and Birch Creek limestone at the base. The Tallant sandstone is a fine to medium grained sandstone with alternating shale layers. Berea sandstone is composed of fine to very fine sub-angular and well sorted sands. The core samples were cut parallel to the bedding plane from the outcrop rock samples with a core bit using water as the cutting fluid. These core plugs were washed out and dried in an oven at 80 ^{o}C (176 ^{o}F). Later the dried samples were weighed. A Ruska gas permeameter was used to measure gas permeability. Values of permeability given in Table 3 are the extrapolated liquid permeability values from Klinkenberg plots (gas permeability versus 1/mean pressure). Diffusion measurements were then run using a pair of helium and nitrogen gases. Porosity was then measured using a vacuum desiccator. The desiccator was evacuated for twenty four hours. The core samples were then saturated with 1.5 percent NaCl and 0.5 percent KCl brine. The core samples were kept immersed for a few hours to insure complete saturation. Four-electrode measurements were then conducted to obtain resistivity-formation-factor values. These core samples were then placed in a Beckman centrifuge to generate air-brine capillary-pressure data. A detailed description of these diffusion, electrical, and capillary-pressure measurements follows next.

Diffusion Measurements

An apparatus to measure the effective diffusion coefficient (D_e) through core samples has been used. The apparatus consists of a core holder, two precision regulators, a gas chromatograph, a recorder, a

nitrogen tank, and a helium tank. The flow system was designed according to the method developed by Weisz (1957), with some changes to permit in-line calibration and better baseline stability (Perkins and Johnston, 1963). A 3.35 cm long by 1.9 cm diameter core and two copper end pieces of the same diameter, placed against the core, are mounted in surgical rubber tubing. The effective diffusion coefficient is measured by the counter-current flow of two gases through the core while maintaining the same pressure at both ends of the core so that the pressure drop across the two faces of the core is zero. The two gases used were nitrogen and helium. Nitrogen (test gas) flows through the porous rock sample while helium acts as the carrier gas. After a baseline was established, carrier gas was allowed to flow at one face of the core and test gas at the other face. Flow of the test gas was set so that the differential manometer indicated the same pressure on both ends of the core. The pressure on both sides of the core holder is kept constant by precision pressure regulators. Equilibrium was indicated by a steady signal on the strip chart recorder. The concentration of the effluent gases are measured using gas chromatograph with a thermal conductivity detector. Experimental data of molecular diffusion were obtained from analysis of the effluent concentration of nitrogen in the helium stream.

Molecular diffusion through porous material is typically described as either bulk, or Knudsen diffusion. Bulk diffusion occurs when the pore diameter of the rock is large in comparison to the mean free path of the gas molecules. Molecular transport through pores which are small in comparison to the mean free path of the gas is described as Knudsen-type diffusion. For this type, molecules collide more often with the pore walls than with other molecules. As a result of the frequent collisions with the wall of the pore, the transport of the molecule is impeded. As suggested by Wheeler (1951), Knudsen diffusion may be considered when the mean free path of the diffusing gas is approximately less than 10 times the radius of the pore. The mean-free-path is the average distance a molecule travels before it collides with a surface, or with another molecule. Wheeler, therefore, sets a pore radius of one μm as the limit at which bulk diffusion alone will occur and a pore radius of 10^{-2} μm for complete Knudsen diffusion. Bulk and Knudsen diffusion may occur simultaneously in pores with radii between 10^{-2} μm and one μm. The estimated pore sizes for the 14 sandstones used in this work show that most of the pores have radii greater than one μm; hence, the contribution from Knudsen diffusion may be considered negligible. Bulk diffusion takes place in the absence of fluid flow if a concentration gradient exists between two miscible phases in porous media.

Electrical Measurements

The four-electrode technique has been used for resistivity measurements to avoid polarization and other contact resistance effects known to be associated with the use of the two-electrode method. The latter technique consists of mounting the sample between two metal disc electrodes through which a constant current of known magnitude flows. Knowledge of the current and voltage between the two electrodes and the geometry of the core sample suffices to compute its resistivity. Another two-electrode method widely used employs the Wheatstone Bridge. A major drawback of these two-electrode techniques, however, is the development of contact resistance between the metal disc electrodes and the core sample. This contact resistance makes the measured resistivity values enormous. These contact resistances at the electrodes are particularly likely to occur at low water saturation and in oil-wet systems (Sharma et al., 1991).

In addition to the two metal disc electrodes, the four-electrode technique requires two other probes or electrodes that are separate from the current electrodes. Measurement of the resistivity is accomplished through knowledge of the voltage drop across the two voltage probes, distance between the two probes, cross-sectional area of the core sample, and the magnitude of current flowing through the core. The four-electrode technique allows no influence of contact resistance at the current electrodes since it measures resistivity of a portion of the sample between the two voltage probes. Also, the effect of contact resistance at the voltage probes is effectively eliminated because the voltage between the voltage probes is measured with a very high internal impedance electronic voltmeter. A typical value for this internal impedance is 10^7 ohms (Garrouch, 1997). This high impedance draws very little current from the rock through the voltage probes, minimizing polarization effects and chemical reactions, which may cause electrode resistance to develop.

Capillary-Pressure Measurements

A Beckman centrifuge was used to collect air-brine displacement data. The speed of the centrifuge was increased by fixed increments. Meanwhile, the volume of the displaced brine was read from the calibrated polycarbonate tubes through a window in the centrifuge door with the aid of a synchronized strobe when the saturation equilibrium had been reached. The time required to reach equilibrium is a function of fluid viscosity, length and pore size distribution of the core sample. The time increment between steps was approximately 15 minutes for the Elgin, Tallant and Okesa sandstone samples, and 30 minutes for Berea samples. The centrifuge acceleration was increased until fluid could no longer be expelled from the core samples. The Hassler-Brunner technique (Hassler and Brunner, 1945) was used to convert the centrifuge data of collected water versus rpm into capillary pressure versus water saturation at the inlet facet ("top face") of the core sample. The method developed by Ritter and Drake (1945) is used to transform the capillary-pressure curves into distribution functions (Collins, 1990). The method is illustrated as follows: If the porous medium is considered as a collection of pores having some radii distribution, then equations can be derived for relating this distribution function to the capillary pressure-saturation relationship. The capillary pressure for a cylindrical tube of diameter, D_i is given by

$$P_c(D_i) = \frac{4\,s\cos q}{D_i}\,, \tag{2}$$

and the relation between P_c and the distribution function $\alpha(D_i)$ is given by

$$a(D_i) = 2\frac{P_c V_p}{D_i}\frac{dS_{nw}}{dP_c}\,. \tag{3}$$

For one bulk volume, i.e. $V_b = 1\ cm^3$, Equation (3) becomes

$$a(D_i) = 2\frac{P_c f}{D_i}\frac{dS_{nw}}{dP_c} \tag{4}$$

According to Collins (1990), $\alpha(D_i)dD_i$ is the fraction of the pore volume contributed by pore throats with diameters varying between D_i and D_i+dD_i. In these equations D_i is the pore entry diameter, and V_p is the rock pore volume. A typical curve of this type is shown in Figure 1. Here the distribution function is based on the capillary-tube-model assumption. Therefore, the area under the curve is a measure of the pore volume that controls flow through porous media, namely that of the pore throats. As shown in Table 3 the area under the distribution function, (a_α), which is given by

$$a_a = \int_{D_{min}}^{D_{max}} a(D)dD\,, \tag{5}$$

correlates positively with the rock sample permeability.

RESULTS AND DISCUSSION

We calculated the coefficient of diffusion by comparing the experimental data with numerical finite difference solutions of the diffusion equation (Gulsen and Smith, 1975). The molecular gas diffusion at the transient state is described by Fick's second law of diffusion through porous media as :

$$f\frac{\partial C}{\partial t} = D_e\frac{\partial^2 C}{\partial x^2} \qquad (6)$$

Equation (6) was solved by Crank-Nicholson numerical technique using the following initial and boundary conditions:

C = 0,	t = 0,	$0 \le x \le L$
C = 1,	x = 0,	t > 0
$\frac{\partial C}{\partial x} = 0$,	x = L,	t > 0

A Fortran code was developed to determine the effective molecular diffusion coefficient. The concentration profile was calculated by choosing various arbitrary values of D_e. Calculated concentration profiles were compared with that of experimental data to obtain the values of D_e. The closest fit gives the particular value of D_e for a given rock sample. A sample of the graphical results of this analysis is shown in Figure 2 for Elgin sandstone rock sample. The values of diffusion coefficients calculated from these matched curves are shown in Table 3. The molecular diffusion coefficient, D_m, was read from the International Critical Tables, and was taken as 0.696 cm^2/sec (Klinkenberg, 1951).

Tortuosity values have been calculated twice independently using the effective diffusivity data, and the electrical conductivity data. Values of tortuosity obtained have been compared for analogous electrical and diffusion models. For instance Peterson (1858) diffusion model is analogous to Cornell and Katz (1953) electrical model. Brakel and Heertjes (1974) diffusion model is analogous to Pirson's (1983) electrical model. The analogy between diffusion and electrical conductivity in porous media has been recognized by a few investigators like Brigham et al. (1961), Grane and Gardner (1961), and van der Poel (1962). For those electrical conductivity models that do not have a published diffusion analog model, we have constructed an analogous model based on the proven similarity between the resistivity formation factor (F) and the ratio (D_m/D_e). For Brakel and Heertjes model and Petersen diffusion models for tortuosity, a value of one has been assumed for the constrictivity factor δ. Figures 3 and 4 show tortuosity values calculated using electrical conductivity models and diffusion models, respectively. With the exception of Faris model (Perkins, 1963), and Dogu and Smith's (1975), tortuosity values for sandstone rocks seem to range between approximately 2 and 3. Figure 5 compares tortuosity values obtained from a particular diffusion model with its corresponding electrical model analog. The average absolute relative difference between Pirson's model and its analog Brakel and Heertjes model was the smallest for all core samples $(\%difference = 8.5 \pm 4.9)$. Wyllie electrical model for tortuosity and its analog appeared to give the highest average absolute percentage relative difference $(\%difference = 16.3 \pm 8.9)$.

The agreement between diffusion-derived tortuosities (using Brakel and Heertjes model) with those obtained from electrical measurements using Pirson's model may indicate the ability of these models to mimic the physics controlling tortuous flow behavior in sandstone rocks. To check the validity of this statement we constructed the values of permeability using the diffusion-derived tortuosity values using the simple capillary-tube model given by

$$k = h\frac{\bar{r}^2 f}{8t^2}. \qquad (7)$$

The average pore radius is half of the first statistical moment around the origin of the distribution function divided by porosity, and η is a pore geometric factor. The larger the value of a_α is, the larger the permeability value becomes. It is found that an estimate of the pore geometric factor η that is proportional to the area under the distribution function (a_α), and inversely proportional to the tortuosity squared, allows the above permeability model to perfectly match the measured permeability values (Table 3). The average absolute relative error between measured permeability values and those estimated using the model presented

by Equation (7) is 6.72% with a standard deviation of 6.57%. These results apply for tortuosity values obtained from Brakel and Heertjes model. The relationship between η and a_α is given by

$$h = \frac{10a_\alpha}{t^2} \tag{8}$$

This relationship between η, a_α, and τ appears to be deterministic, and not merely a statistical inference. This may be true since permeability given by Equation (7) appears to increase as the parameter a_α increases, and appears to decrease as the tortuosity increases. The best permeability match occurs for tortuosity values estimated using Brakel and Heertjes model, which is analogous to Pirson's electrical model. These results reinforce the validity of Pirson's model and Brakel and Heertjes model for estimating sandstone rock tortuosity.

CONCLUSIONS

Diffusion, electrical and capillary pressure measurements were performed on a suite of 14 sandstone rock samples for the purpose of estimating their tortuosity values. These measurements allowed to further verify the assumption that electrical and molecular diffusivities are equivalent. Tortuosity values calculated from diffusion measurements (using Brakel and Heertjes model) matched reasonably well with those values estimated using Pirson's electrical model. These results indicate the superiority of the latter model over a large number of formation-factor based models. This statement is even supported by the ability of a simple-capillary tube model to duplicate the measured permeability values when using these estimated tortuosity values. The capillary tube model has been adjusted by a well defined pore geometric factor that is proportional to the volume of the pore throats controlling fluid flow through porous media, and inversely proportional to the tortuosity squared.

NOMENCLATURE

a_α	area under the distribution function
a_{vb}	specific surface area of pore-bridging cement
a_{vl}	specific surface area of pore-lining cement
a_{vf}	specific surface area of pore-filling cement
C	dimensionless concentration
C_{DP}	coefficient of variation
$\overline{D}$	average pore diameter
D_e	effective molecular diffusion coefficient
D_i	pore-entry diameter
D_m	molecular diffusion coefficient
D_{min}	minimum rock pore-entry diameter
D_{max}	maximum rock pore-entry diameter
$\overline{D}_p$	average grain size
k_{est}	estimated permeability using tortuosity from Brakel and Heertjes model
k_m	measured permeability
L	core-sample length
P_c	capillary pressure
P_b	amount of pore-bridging cement, a fraction of total solid volume
P_d	threshold pressure
P_f	amount of pore-filling cement, a fraction of total solid volume

P_l	amount of pore-lining cement, a fraction of total solid volume
$\bar{r}$	average pore-entry radius
S_{nw}	non-wetting phase saturation
t	time
x	distance

Greek Symbols

$\alpha(D_i)$	distribution function
δ	constrictivity factor
ϕ	rock porosity
ϕ_o	clay-free rock porosity
h	pore geometric factor
σ	interfacial tension
θ	contact angle
τ	tortuosity

REFERENCES

1. Brakel, J. V., and Heertjes, P.M., Analysis of diffusion in macroporous media in terms of porosity, a tortuosity and a constrictivity factor, *Int. J. Heat Transfer*, (1974), **v. 17**, p. 1093-1103.
2. Brigham, W.E., Reed, P.W., and Dew, J.N., Experiments on mixing during miscible displacement in porous media, *Soc. Pet. Eng. J.*, (1961), **v. 1**, no. 2, p. 221-226.
3. Collins, R.E., Flow of Fluids Through Porous Media, Research and Engineering Consultants Inc., Englewood (1990), Colorado, p. 31-33.
4. Cornell, D., and Katz, D.L., Flow of gases through consolidated media, *Industrial and Engineering Chemistry*, (1953), **v. 45**, no. 10, p. 2145-2152.
5. Dogu, G., and Smith, J.M., A dynamic method for catalyst diffusivities, *AIChE Journal*, (1975), **v. 21**, no. 1, p. 58-61.
6. Garrouch, A.A., Use of the saturation exponent as a measure for quantifying reservoir rock wettability, *In Situ*, (1997), **v. 20**, no. 4, 413-438.
7. Garrouch, A.A., and Lababidi, H.M.S., An inverted petrophysical model for shaly sands, *In Situ*, (1995), **v. 19**, no. 2, p. 125-153.
8. Grane, F.E., and Gardner, G.H.F., Measurements of transverse dispersion in granular media, *Journal of Chem. Eng. Data*, (1961), **v. 26**, no. 2, 283.
9. Gulsen, D., and Smith, J.M., A dynamic method for catalyst diffusivities, *AIChE Journal*, (1975), **v. 21**, no. 1, p. 58-61.
10. Hassler, G.L., and Brunner, E., Measurement of capillary pressures in small core samples, *Trans. AIME*, (1945), **v. 160**, no. 3, p. 114-123.
11. Hedley, W. H., Lavacot, F.J., Wang, S.L., and Armstrong, W.P., Accessibility of surface to gases diffusing inside macroporous media, *AIChE Journal*, (1966), **v.12**, no. 2, p. 321-327.
12. Klinkenberg, L.J, Analogy between diffusion and electrical conductivity in porous rocks, *Geol. Soc. of Am. Bull.*, (1951), **v.62**, no. 4, p. 559-564.
13. Panda, M.N., and Lake L.W., A physical model of cementation and its effects on single-phase permeability, *AAPG Bulletin*, (1995), **v. 79**, no. 3, p. 431-443.
14. Perkins, T.K., and Johnston, O.C., A review of diffusion and dispersion in porous media, *Soc. Petroleum Eng. J.*, (1963), **v. 3**, no.1, p. 70-84.
15. Petersen, E.E., Diffusion in a pore of varying cross-section, *AIChE Journal*, (1958), **v. 4**, no. 3., p. 343-345.
16. Pirson, S.J., Geologic Well Log Analysis, Gulf Publishing, Houston, TX (1983), p. 136-138.
17. Ritter, H.L, and Drake, L.C., Pore size distribution in porous materials, *Industrial and Engineering Chemistry Journal*, (1945), **v. 17**, no. 12, p. 782-791.

18. Savins, J.G., Non-Newtonian flow through porous media, *Industrial and Engineering Chemistry Journal*, (1969), **v. 61**, no. 10, p. 18-47.
19. Sharma, M. M., Garrouch, A. A. , and Dunlap, H. F., Effects of wettability, pore geometry, and stress on electrical conduction in fluid-saturated rocks, *The Log Analyst*, (1991), **v. 32**, no. 5, p. 511-526.
20. van der Poel, C., Effect of lateral diffusivity on miscible displacement in horizontal reservoirs, *Soc. Pet. Eng. J.*, (1962), **v. 2**, no.6, 317.
21. Weisz, B.P., Diffusivity of porous particles, *Neue Folge, Bdg.*, (1957), **v. 11**, no. 4, p. 1-15.
22. Wheeler, A., Advances in catalysis and related subjects v. III, Academic press, New York (1951), p. 249-327.
23. Winsauer, W.O., Shearin, H.M., Masson, P.H., and William, M., Resistivity of brine-saturated sands in relation to pore geometry, *Bull. Amer. Assoc. Petrol. Geol.*, (1952), **v. 36**, no. 2, p. 253-277.
24. Wyllie, M.R. J., and Spangler, M.B., Application of electrical resistivity measurements to problem of fluid flow in porous media, *AAPG Bull.*, (1952), **v. 36**, no.2, p. 359-403.

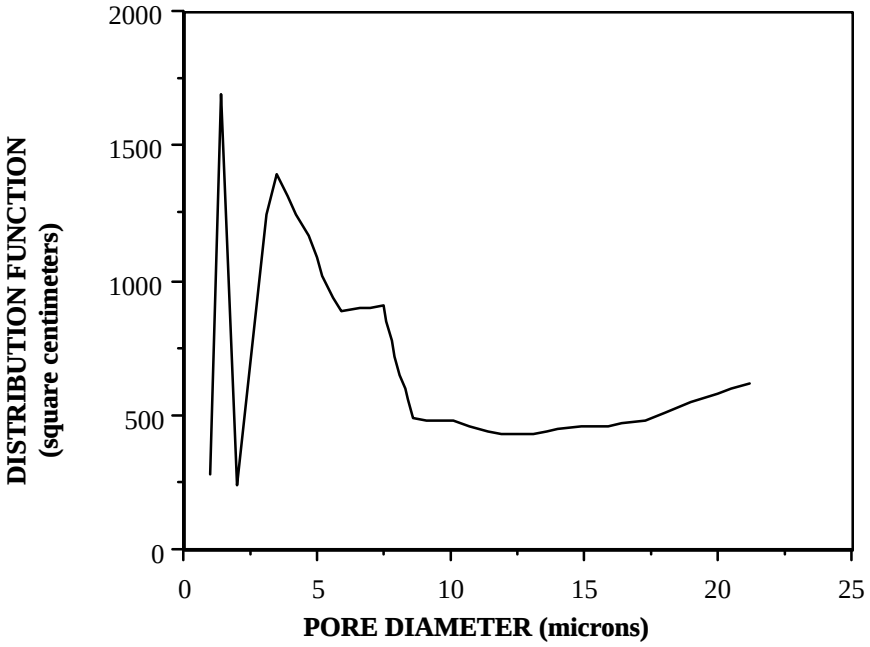

Figure 1: Distribution function for Tallant sandstone rock sample.

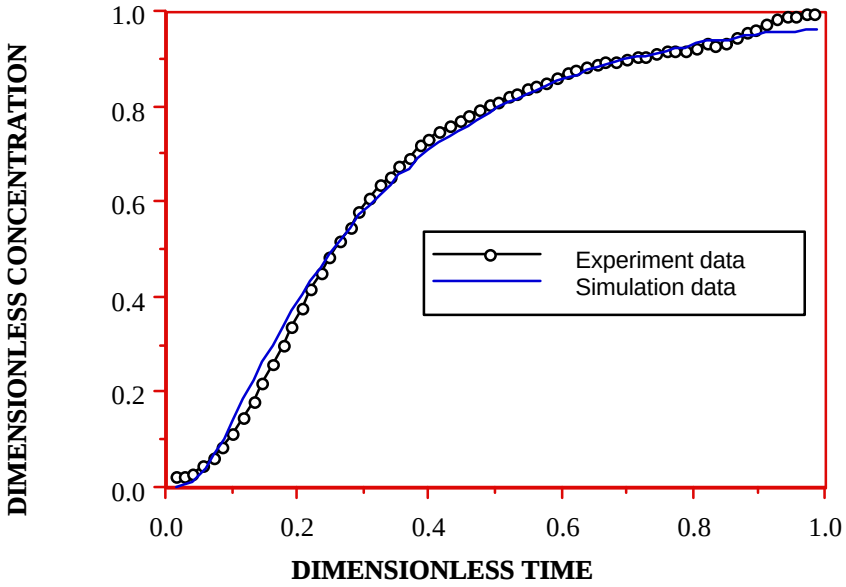

Figure 2: Matching the dimensionless concentration profile for Elgin sandstone.

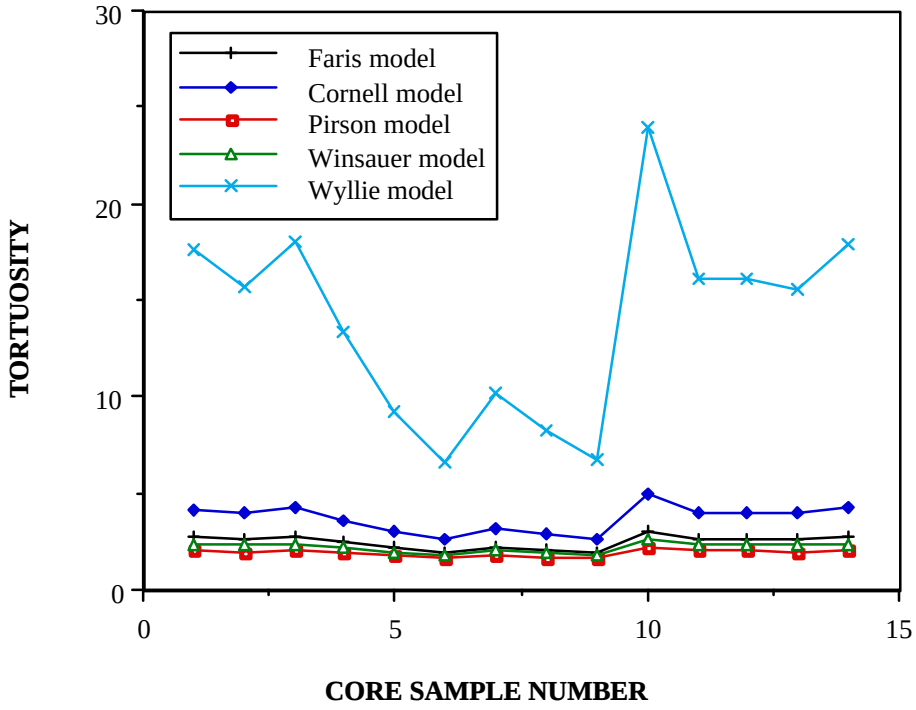

Figure 3: Tortuosity derived from electrical measurements for all sandstone core samples used.

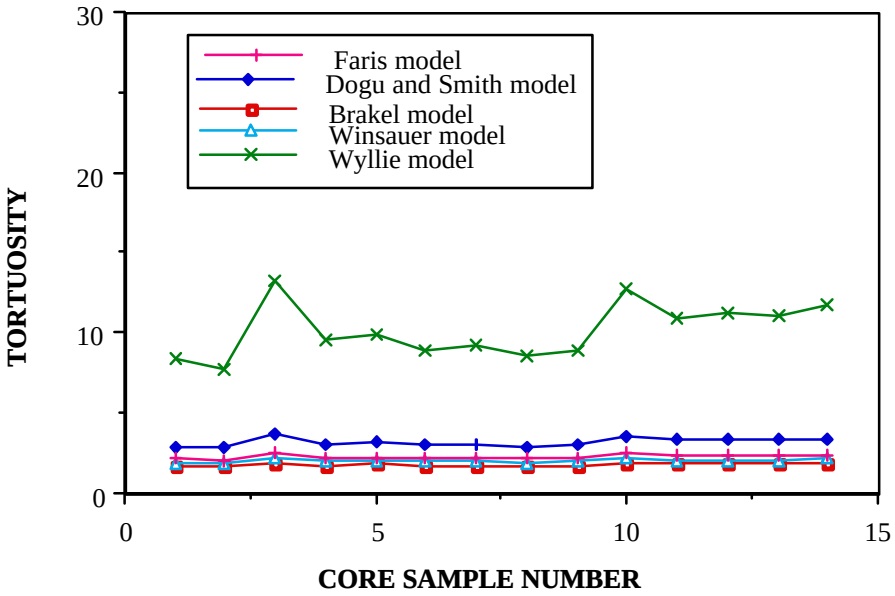

Figure 4: Tortuosity derived from effective diffusivity measurements for all sandstone cores used.

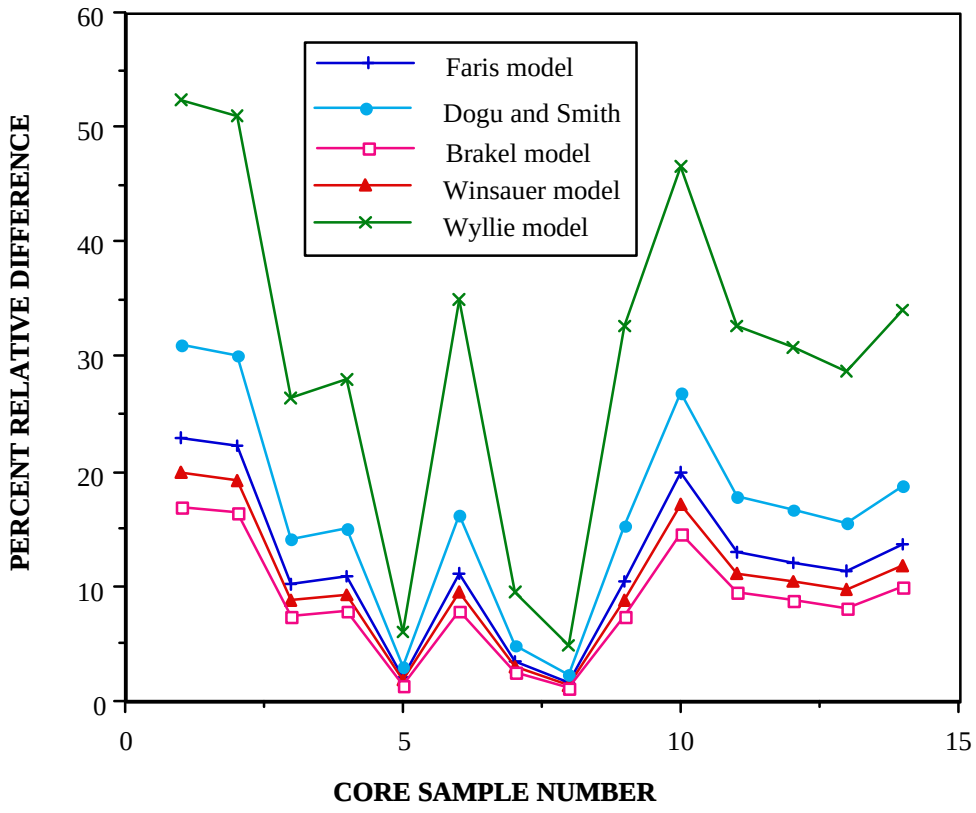

Figure 5: Percent relative difference between tortuosity derived from effective diffusivity measurements and tortuosity derived from electrical conductivity measurements for all sandstone core samples used.

Table 1: Electrical resistivity models for tortuosity.

Author	Year	Model
Wyllie and Spangler	1952	$t = (\mathrm{F}f)^2$
Winsauer et al.	1952	$t^2 = (\mathrm{F}f)^{1.2}$
Cornell and Katz	1953	$t = \mathrm{F}f$
Faris et al.	1954	$t^2 = (\mathrm{F}f)^{\mathrm{n}}$; $1.2 \le \mathrm{n} \le 1.41$
Pirson	1983	$t^2 = (\mathrm{F}f)$

Table 2: Molecular diffusivity models for tortuosity.

Author	Year	Model
Wyllie and Spangler	1952	$t = \left(\frac{f\,\mathrm{D_m}}{\mathrm{D_e}}\right)^2$
Winsauer et al.	1952	$t^2 = \left(\frac{f\,\mathrm{D_m}}{\mathrm{D_e}}\right)^{1.2}$
Petersen	1958	$\frac{\mathrm{D_e}}{\mathrm{D_m}} = \frac{fd}{t}$
Faris et al.	1954	$t^2 = \left(\frac{f\,\mathrm{D_m}}{\mathrm{D_e}}\right)^{1.41}$
Hedley et al.	1966	$t = \frac{f_e\left(\frac{f_f}{f_p}\right)}{\mathrm{D_e}}\mathrm{ND_m}$
Brakel and Heertjes	1974	$t = \sqrt{\frac{fd}{\mathrm{D_e}/\mathrm{D_m}}}$
Dogu and Smith	1975	$t = \frac{f\,D_m}{D_e}$

Table 3: Petrographic properties of the sandstone rock samples.

Sample	Count	ϕ (%)	$\overline{D}$ (μm)	D_e (cm^2/sec)	F	a_α (cm^3)	k_{est} (md)	k_m (md)
Berea-A	1	19.3	6.9	0.04650	21.68	0.238	82.9	83
Berea-B	2	20.5	6.4	0.05147	19.33	0.404	140	126
Berea-C	3	19.1	6.2	0.03634	22.32	0.544	95	85
Okesa-A	4	24.6	6.6	0.05530	14.83	0.99	351	315
Okesa-B	5	26.0	7.3	0.05781	11.69	1.08	483	487
Tallant-A	6	27.1	8.7	0.06312	9.491	1.03	749	703
Tallant-B	7	25.7	9.2	0.05871	12.46	1.07	795	637
Tallant-C	8	26.5	8.5	0.06281	10.82	1.02	718	667
Tallant-D	9	27.1	8.4	0.06297	9.593	1.00	676	651
Elgin-A	10	22.4	15	0.04368	21.82	1.27	1590	1715
Elgin-B	11	24.2	18	0.05109	16.60	1.11	2538	2502
Elgin-C	12	24.2	16	0.05037	16.60	1.20	2131	2060
Elgin-D	13	23.9	16	0.04997	16.50	1.22	2131	2156
Elgin-E	14	23.5	16	0.04755	18.04	1.28	2064	2151